energies

MDPI

Article

Experimental Investigation of Enhanced Oil Recovery Mechanism of CO_2 Huff and Puff in Saturated Heavy Oil Reservoirs

Xiaorong Shi [1], Qian Wang [2], Ke Zhao [3], Yongbin Wu [2,*], Hong Dong [1], Jipeng Zhang [4] and Ye Yao [5]

[1] Research Institute of Petroleum Exploration and Development, Xinjiang Oilfield Company, PetroChina, Karamay 834000, China; shixiaor@petrochina.com.cn (X.S.); hongdong@petrochina.com.cn (H.D.)
[2] Research Institute of Petroleum Exploration and Development, PetroChina, Beijing 100083, China; wangqian66@petrochina.com.cn
[3] Heavy Oil Recovery Branch of Xinjiang Oilfield Company, PetroChina, Karamay 834000, China; zhaoke66@petrochina.com.cn
[4] School of Energy Resources, China University of Geosciences, Beijing 100083, China; 18152696912@163.com
[5] School of Accounting, Shanghai Lixin Accounting and Finance College, Shanghai 201600, China; 18154899389@163.com
* Correspondence: wuyongbin@petrochina.com.cn

Abstract: Due to the significance of carbon utilization and storage, CO_2 huff and puff is increasingly receiving attention. However, the mechanisms and effects of CO_2 huff and puff extraction in medium to deep saturated heavy oil reservoirs remain unclear. Therefore, in this study, by targeting the medium to deep saturated heavy oil reservoirs in the block Xia of the Xinjiang oil field, measurements of physical properties were conducted through PVT analysis and viscosity measurement to explore the dissolution and diffusion characteristics of CO_2-degassed and CO_2-saturated oil systems. Multiple sets of physical simulation of CO_2 huff and puff in medium to deep saturated heavy oil reservoirs were conducted using a one-dimensional core holder to evaluate the EOR mechanism of CO_2 huff and puff. The results demonstrate that the solubility of CO_2 in degassed crude oil is linearly correlated with pressure. Higher pressure effectively increases the solubility of CO_2, reaching 49.1 m^3/m^3 at a saturation pressure of 10.0 MPa, thus facilitating oil expansion and viscosity reduction. Meanwhile, crude oil saturated with CH_4 still retains the capacity to further dissolve additional CO_2, reaching 24.5 m^3/m^3 of incremental CO_2 solubilization at 10.0 MPa, and the hybrid effect of CO_2 and CH_4 reduces oil viscosity to 1161 mPa·s, which is slightly lower than the pure CO_2 dissolution case. Temperature increases suppress solubility but promote molecular diffusion, allowing CH_4 and CO_2 to maintain a certain solubility at high temperatures. In terms of dynamic dissolution and diffusion, the initial CO_2 dissolution rate is high, reaching 0.009 $m^3/(m^3 \cdot min)$, the mid-term dissolution rate stabilizes at approximately 0.002 $m^3/(m^3 \cdot min)$, and the dissolution capability significantly decreases later on. CO_2 exhibits high molecular diffusion capability in gas-saturated crude oil, with a diffusion coefficient of 8.62×10^{-7} m^2/s. For CO_2 huff and puff, oil production is positively correlated with the CO_2 injection rate and the cycle injection volume; it initially increases with the extension of the soak time but eventually decreases. Therefore, the optimal injection speed, injection volume, and soak time should be determined in conjunction with reservoir characteristics. During the huff and puff process, the bottom hole pressure should be higher than the bubble point pressure of the crude oil to prevent gas escape. Moreover, as the huff and puff cycles increase, the content of saturates in the oil rises, while those of aromatic, resin, and asphaltene decrease, leading to a gradual deterioration of the huff and puff effect. This study provides a comprehensive reference method and conclusions for studying the fluid property changes and enhanced recovery mechanisms in medium to deep heavy oil reservoirs with CO_2 huff and puff.

Keywords: medium to deep saturated heavy oil; CO_2 huff and puff; dissolution and diffusion; EOR mechanism

check for updates

Citation: Shi, X.; Wang, Q.; Zhao, K.; Wu, Y.; Dong, H.; Zhang, J.; Yao, Y. Experimental Investigation of Enhanced Oil Recovery Mechanism of CO_2 Huff and Puff in Saturated Heavy Oil Reservoirs. *Energies* **2024**, *17*, 6391. https://doi.org/10.3390/en17246391

Academic Editor: Dameng Liu

Received: 7 September 2024
Revised: 1 November 2024
Accepted: 26 November 2024
Published: 19 December 2024

Copyright: © 2024 by the authors. Licensee MDPI, Basel, Switzerland. This article is an open access article distributed under the terms and conditions of the Creative Commons Attribution (CC BY) license (https://creativecommons.org/licenses/by/4.0/).

1. Introduction

The overall distribution of oil resources in the world shows that conventional crude oil accounts for only 30% of the global oil resources, and the remaining 70% are unconventional crude oil, including heavy oil, ultra-heavy oil, asphalt, tight oil, and oil shale oil [1]. China is the fourth largest global heavy oil producer after the United States, Canada, and Venezuela [2]. Heavy oil fields in China are mainly concentrated in the Liaohe oilfield, the Bohai Bay oilfield, the ShengLi oilfield, the Karamay oilfield, and the Henan oilfield.

At present, steam stimulation and steam flooding are mature technologies for heavy oil thermal recovery, which is mainly suitable for the development of medium-shallow heavy oil reservoirs [3]. However, due to the limitation of heat loss, the reservoir depth developed by foreign thermal recovery is generally less than 700 m [4]. The buried depth of heavy oil reservoirs in China is generally deep, and the range of variation is large [5]. The resources of heavy oil reservoirs in Liaohe Oilfield with a buried depth of 900~1300 m account for 34% of the total resources of heavy oil, and the resources with a buried depth greater than 1300 m account for 34% of the total resources [6]. Most of the heavy oil reservoirs in eastern China are buried more than 800 m, and the deepest can reach 1700 m. The buried depth of Tuha and Tarim heavy oil in the western part of Tuha is more than 2000 m, and the deepest can reach more than 5000 m. The heavy oil reservoirs in the Bohai Sea are mainly distributed at the depth range of 1000~2000.

Steam thermal recovery technology is an important means of exploiting heavy oil reservoirs. However, for medium to deep heavy oil reservoirs, steam thermal recovery technology has its limitations. On the one hand, the steam injection pressure is too high, and the steam quality is reduced; on the other hand, the heat loss is greater, the steam enthalpy value is low, and it cannot effectively heat the reservoir, which can lead to a poor reservoir development effect, and the economic benefit is low [7–9].

The permeability and porosity of medium to deep heavy oil reservoirs are low; therefore, the heat loss of steam injected from the wellhead to the bottom of the well is great, resulting in a small radial sweep radius of steam, which is difficult to effectively develop and use [10]. The conventional solution is to use gas, solvent, urea, and other common media to assist steam huff and puff to improve the steam sweep range and reduce the viscosity of crude oil. However, the oil production is only 100~200 tons in a single cycle, and the output–input is relatively low [11,12].

CO_2 gas-assisted oil recovery was industrialized in North America in 1952. Compared with other non-hydrocarbon media, CO_2 has a better miscibility with crude oil, which can reduce the interfacial tension between crude oil molecules. At the same time, CO_2 dissolves in crude oil and expands its volume, which greatly reduces the viscosity of crude oil and significantly improves the fluidity of crude oil. In the development of heavy oil, the use of CO_2 to improve reservoir recovery technology is mostly used for ordinary heavy oil huff and puff, and it achieves a good oil increase effect, as the oil change rate is 0.18~1.31 [13,14]. Since the concept of enhanced oil recovery through CO_2 huff and puff was put forward, many scholars at home and abroad have carried out a lot of research on the mechanism of enhanced oil recovery through field application and laboratory experiments. Haskin et al. [15] carried out CO_2 huff and puff laboratory experiments on crude oils with different viscosities and evaluated the field tests of 28 wells in 12 oilfields in eastern and southern Texas. It is considered that crude oil expansion and dissolution viscosity reduction are important mechanisms for improving oil recovery. In the field test of CO_2 huff and puff in the South Louisiana reservoir [16], when the viscosity of CO_2 in the reservoir decreases, the production rate increases, which indicates that viscous fingering has a positive effect on the process of CO_2 huff and puff. At the same time, it is found that CO_2 can extract the light hydrocarbon components in crude oil, thereby increasing the single well production. Schenewerk et al. [17] found that CO_2 huff and puff can significantly change the distribution of oil saturation near the wellbore and greatly reduce the water content in the produced fluid. Wehner [18] analyzed the effect of a CO_2 huff and puff test in a New Mexico reservoir and found that the mechanism of crude oil expansion and viscosity reduction plays an

important role in the generation of the initial daily oil production peak, but the oil increase effect lasts for a short time, and the trap gas saturation is the main factor leading to the continuous oil increase of CO_2 huff and puff in light oil reservoirs. Wang et al. [19] carried out CO_2 huff and puff laboratory experiments. The results show that the dissolution of CO_2 in crude oil can reduce the oil–water interfacial tension, increase the formation pressure and energy near the wellbore, and form a dissolved gas drive after well opening, thus increasing the single well production.

In recent years, a CO_2 storage fracturing test has been carried out in the heavy oil block of the middle–deep low permeability layer, such as in Jidong Oilfield. CO_2 storage fracturing is a kind of water-free formation stimulation improvement measure using liquid CO_2 as fracturing medium. Compared with conventional hydraulic fracturing, it has the characteristics of a no-water phase, no residue, and rapid flowback. For water-sensitive and water-locked formation, the characteristics of the water-free phase of CO_2 storage fracturing mean that it does not cause the clay in the formation to expand and migrate and block the seepage channel after construction, so it can be well-adapted to the water-sensitive and water-locked formation. Compared to the filter cake formed on the fracture surface by conventional hydraulic fracturing, the use of liquid CO_2 does not cause a decrease in reservoir and fracture permeability. In the flowback process after fracturing, liquid CO_2 changes from liquid to gas, which can realize rapid flowback, solve the problem of difficult flowback after pressure in a low-permeability reservoir, and realize rapid flowback after pressure and be put into production [20,21].

The middle–deep and low-permeability heavy oil resources in Xinjiang are abundant, and the proven untapped controlled geological resources are more than one-third, which have the characteristics of deep burial, poor physical properties, and high viscosity. At present, the conventional cold production is not more than 15%, the single well production is low, and the conventional development recovery rate is less than 5%. The target study area is the Xia block in Xinjiang. The permeability is approximately 357.9 mD, but the oil viscosity is approximately 1250 mPa·s at a reservoir temperature of 33.35 °C. The reservoir is a saturated reservoir with a gas cap, and the original dissolved gas–oil ratio is 16.5 m^3/m^3 at the original pressure of 7.3 MPa. A small range of CO_2 storage fracturing has been implemented in the target area, and good results have been obtained. To study the variation law of reservoir fluid physical properties after CO_2 injection in gas-bearing reservoirs, in this paper, a high-temperature and high-pressure PVT instrument and rheometer are used to carry out CO_2 dissolution and molecular diffusion experiments under different conditions, and a one-dimensional core holder is used to conduct multiple sets of physical simulation of CO_2 huff and puff in medium to deep saturated heavy oil reservoirs. The competitive dissolution of CO_2 and CH_4, the molecular diffusion distance and the viscosity reduction effect of CO_2 in gas-bearing reservoirs, and the EOR effect of CO_2 huff and puff were studied. This paper provides a reference for the successful application and efficient development of large-scale CO_2 storage fracturing and subsequent CO_2 huff and huff.

2. Experimental Methodology

2.1. Dissolution and Diffusion

The dissolution and diffusion of CO_2 in gas-bearing and degassed crude oil are important parameters to reflect the development effect of CO_2 in heavy oil reservoirs. It is very important to clarify the solubility, diffusion distance, and viscosity change of CO_2 in gas-bearing and degassed crude oil to reveal the feasibility and recovery effect of CO_2 huff and puff in heavy oil reservoirs. Therefore, it is necessary to carry out CO_2 dissolution and diffusion experiments under different conditions.

2.1.1. Experimental Materials

(1) Oil: Heavy oil samples from the X Block of Xinjiang oilfield are prepared for the experiments at a dead oil viscosity and density of 2354 mPa·s and 0.87 g/cm^3 at a

reservoir temperature of 33.35 °C. These are used to saturate the model for all of the experiments.

(2) Gas: CH_4 with a purity of 99.9%, and CO_2 with a purity of 99.9%.

2.1.2. Experimental Apparatus

The purpose of this experiment is to test the physical properties of fluids under various conditions by using a high-temperature and high-pressure PVT analytical instrument from Petrolabs Tech Limited, Beijing, China and RS6000 rheometer from Thermo Fisher Scientific Inc., Carlsbad, CA, USA. Figure 1 shows the schematic diagram of the integrated test device for the PVT analysis and viscosity measurement, and Figure 2 shows the physical diagram of the integrated test device. As shown in Figures 1 and 2, the experimental equipment mainly consists of four parts.

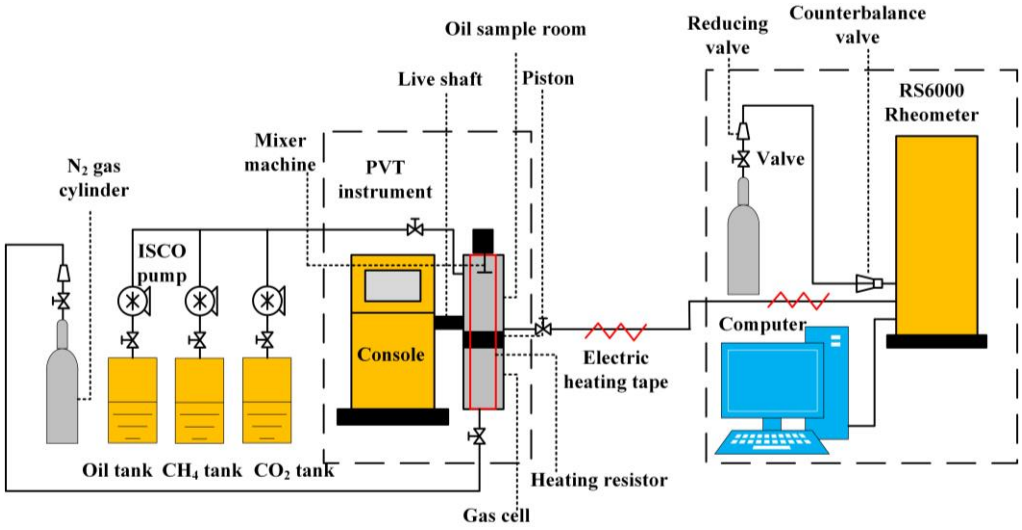


Figure 1. Schematic diagram of integrated test device of PVT analysis and viscosity measurement.



Figure 2. Physical diagram of integrated test device.

(1) Injection unit: Composed of three intermediate containers, three high-pressure ISCO pumps, and a reducing valve, which can inject crude oil and solvent into the PVT instrument test chamber at a constant pressure.

(2) PVT analysis unit: Composed of a console and a high-temperature and high-pressure PVT analysis instrument with a heating layer and an insulation layer. The console is used to control the rheometer and collect data, such as temperature, motor speed, etc. The heating layer and the insulation layer are used to heat the test chamber

and maintain it at a relatively constant temperature to ensure the accuracy of the evaluation experiment.

(3) Pressure control unit: Composed of a high-pressure nitrogen cylinder, which is used to change the pressure of the test chamber of the PVT instrument.

(4) Viscosity measurement unit: Composed of an RS6000 rheometer, a high-pressure nitrogen cylinder, a computer, and a reducing valve. The RS6000 rheometer belongs to a high-temperature and high-pressure rheometer, which is mainly used to study the rheological properties of liquids. Its components include an oil bath, a main engine, a pressure system, and a computer system. The temperature is controlled by a computer. The back-pressure valve is connected directly to the measuring cylinder through the high-pressure pipe. The pressure of the back-pressure valve is controlled by manually adjusting the reducing valve of the high-pressure nitrogen cylinder.

2.1.3. Experimental Scenarios and Procedures

In order to obtain the solubility, diffusion distance, and viscosity change of CO_2 in gas-bearing and degassed crude oil, the following four schemes were studied, and brief descriptions of the experimental steps for different scenarios are also presented.

(1) Experiment of CO_2 solubility and oil viscosity in degassed crude oil at reservoir temperatures and different pressures.

   (a) The tightness of the comprehensive test device was checked;
   (b) The PVT cylinder was placed vertically, the piston in the cylinder was withdrawn to the bottom, and the crude oil of 60% of the volume of the PVT cylinder was injected into the cylinder, followed by vacuuming, heating, and maintaining the reservoir temperature;
   (c) The piston in the cylinder was pushed to gradually increase the pressure of the PVT cylinder, and the change in pressure and volume was recorded. When the pressure reached the reservoir pressure, the oil outlet valve was opened, and the oil sample was transported to the rheometer for the viscosity test;
   (d) The piston in the cylinder was withdrawn to the bottom, a certain amount of CO_2 was injected, the PVT cylinder pressure was adjusted to gradually increase, the pressure and volume were recorded, and the viscosity under reservoir pressure was measured;
   (e) Repeated step (d) and added CO_2 5 times;
   (f) Ended the test, and the test data were processed to calculate the CO_2 solubility and viscosity of the degassed crude oil under different pressures.

(2) Experiment of CO_2 solubility and crude oil viscosity in gas-bearing crude oil at reservoir temperatures and different pressures.

   (a) The tightness of the comprehensive test device was checked;
   (b) The PVT cylinder was placed vertically, the piston in the cylinder was withdrawn to the bottom, and the crude oil of 60% of the volume of the PVT cylinder was injected into the cylinder, followed by vacuuming, heating, and maintaining the reservoir temperature;
   (c) A large amount of CH_4 was injected, and then the PVT cylinder pressure was gradually adjusted to increase, and the pressure and volume were recorded. When the dissolved gas–oil ratio reached the original dissolved gas–oil ratio of the formation, the remaining CH_4 was discharged;
   (d) A certain amount of CO_2 was injected, and then the PVT cylinder pressure was adjusted again to gradually increase, and the pressure and volume were recorded;
   (e) Repeated step (d) and added CO_2 5 times;
   (f) Ended the test, and the test data were processed to calculate the CO_2 solubility and viscosity of the original gas-bearing crude oil under different pressures.

(3) Experiment of CO_2 solubility in gas-bearing crude oil at different pressures and different temperatures.
   (a) The tightness of the comprehensive test device was checked;
   (b) The PVT cylinder was placed vertically, the piston in the cylinder was withdrawn to the bottom, and the crude oil of 60% of the volume of the PVT cylinder was injected into the cylinder, followed by vacuuming, heating, and maintaining the reservoir temperature;
   (c) A large amount of CH_4 was injected, and then the PVT cylinder pressure was gradually adjusted to increase, and the pressure and volume were recorded. When the dissolved gas–oil ratio reached the original dissolved gas–oil ratio of the formation, the remaining CH_4 was discharged;
   (d) It stood for 24 h for the solute to distribute evenly;
   (e) CO_2 was injected from the upper part of the PVT cylinder until the pressure reached the formation pressure, and then the valve was closed and stationary so that CO_2 was gradually dissolved into the crude oil, and the pressure drop process in the cylinder was recorded;
   (f) When the pressure in the cylinder reached equilibrium, the pressure remained unchanged, and the upper part of the undissolved CO_2 was discharged by pushing the piston. The oil discharge valve was opened, and the piston continued to be pushed at different distances to determine the viscosity of the crude oil at different dissolution distances;
   (g) Repeated steps (b), (c), and (d), but the temperatures in step (b) became 80 °C and 120 °C, respectively;
   (h) Ended the test, and the test data were processed to calculate the CO_2 solubility of the original gas-bearing crude oil under different temperatures.

(4) Experiment of CO_2 dissolution rate and diffusion distance in gas-bearing crude oil at reservoir temperatures and different pressures.
   (a) The tightness of the comprehensive test device was checked;
   (b) The PVT cylinder was placed vertically, the piston in the cylinder was withdrawn to the bottom, and the crude oil of 60% of the volume of the PVT cylinder was injected into the cylinder, followed by vacuuming, heating, and maintaining the reservoir temperature;
   (c) The piston in the cylinder was pushed to gradually increase the pressure of the PVT cylinder, and the change in pressure and volume was recorded. When the pressure reached the reservoir pressure, the oil outlet valve was opened, and the oil sample was transported to the rheometer for the viscosity test;
   (d) The piston in the cylinder was withdrawn to the bottom, a certain amount of CO_2 was injected, the PVT cylinder pressure was adjusted to gradually increase, the pressure and volume were recorded, and the viscosity under reservoir pressure was measured;
   (e) Repeated step (d) and added CO_2 5 times;
   (f) Ended the test, and the test data were processed to calculate the CO_2 solubility and viscosity of the degassed crude oil under different pressures.

2.2. CO_2 Huff and Puff Experiment

The gas injection parameters of CO_2 huff and puff have a great influence on the whole development effect. In order to reveal the variation characteristics of the development effect with gas injection parameters, CO_2 huff and puff experiments with different parameter settings were carried out.

2.2.1. Experimental Materials

(1) Water: According to the water from block X of Xinjiang oilfield, simulated water was replicated with a salinity of 8500 mg/L.

(2) Oil: Heavy oil samples from the X Block of Xinjiang oilfield were prepared for the experiments at a dead oil viscosity and density of 2354 mPa·s and 0.87 g/cm^3 at a reservoir temperature of 33.35 °C. These were used to saturate the model for all of the experiments.
(3) Gas: CH_4 with a purity of 99.9%, and CO_2 with a purity of 99.9%.

2.2.2. Experimental Apparatus

Figure 3 shows the schematic diagram of the CO_2 huff and puff device. The experimental equipment mainly consists of four parts.

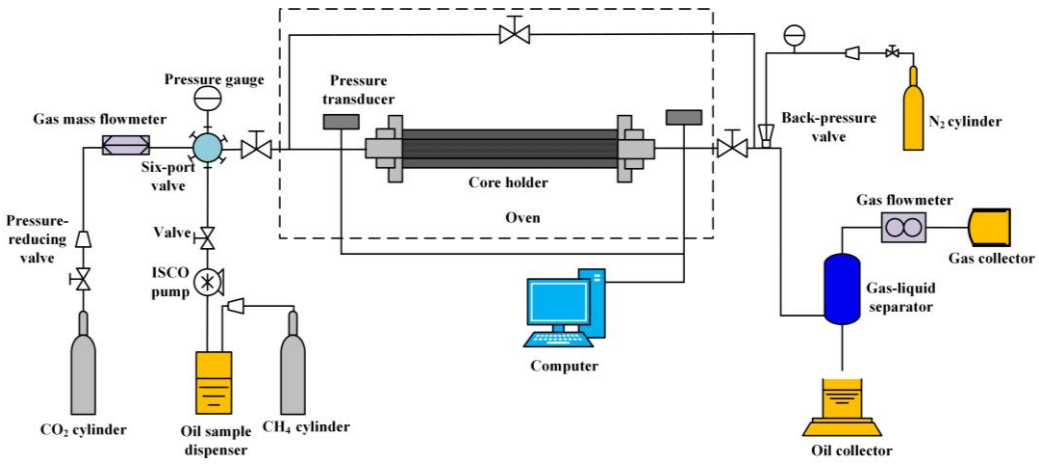


Figure 3. Schematic diagram of CO_2 huff and puff device.

(1) Injection system. It consists of a CO_2 cylinder, a CH_4 cylinder, an oil sample dispenser, two pressure-reducing valves, a gas mass flowmeter, an ISCO high-pressure plunger pump, a six-port valve, and a pressure gauge. The CH_4 cylinder and the oil sample dispenser are used to prepare a gas-bearing oil sample consistent with the reservoir's conditions. The pressure-reducing valve is used to control the injection pressure, and the gas mass flowmeter is used to measure the injection rate. The ISCO high-pressure plunger pump is used to inject gas-bearing oil samples.
(2) Reservoir model. It is composed of an oven with a core holder diameter of 2.5 cm and a length of 50 cm. The oven is heated to control the temperature of huff and puff. The core holder is filled with formation core to simulate the actual reservoir. The measured porosity of the formation core is 28.2%, and the absolute permeability is approximately 358 mD.
(3) Production system. It consists of a back-pressure valve, a N_2 cylinder, a pressure-reducing valve, a pressure gauge, a gas–liquid separator, a gas flowmeter, an oil collector, and a gas collector. The gas–liquid separator is used to separate the produced oil and gas. The gas flowmeter measures the volume of the produced gas.
(4) Data sensing system. It is composed of two pressure transducers and a computer, which can transmit and record pressure data in real time.

2.2.3. Experimental Scenarios

In order to reveal the variation characteristics of the development effect with gas injection parameters, the throughput optimization experiments were carried out for the following four types of gas injection parameters in Table 1.

Table 1. Optimization range of different gas injection parameters in CO_2 huff and puff.

Parameters	Injection Volume	Injection Rate	Soaking Time	Bottom Hole Pressure
Unit	**PV**	**10^2 mL/min**	**min**	**MPa**
Optimization range	0.10	3	60	1.5
	0.15	4	70	2.0
	0.20	5	80	2.5
	0.25	6	90	3.0
	0.30	7	100	3.5
	0.35	8	110	4.0

2.2.4. Experimental Procedures

The following is a brief description of the experimental steps.

(1) The sampler was used to configure the gas-bearing crude oil sample. The back-pressure valve's pressure was adjusted to be consistent with the actual formation pressure.
(2) The core was vacuumized to saturate the water, and then crude oil was injected to establish the initial oil saturation of crude oil.
(3) Depressurization depletion mining was started until no oil was produced.
(4) The first cycle of CO_2 huff and puff was started. After injecting CO_2 into the core, all valves were closed to soak the well so that CO_2 could be fully dissolved and diffused into the formation crude oil. Finally, the back-pressure valve was adjusted to the set production pressure (bottom hole pressure) for production. The first cycle of throughput ended when no oil was produced.
(5) Repeated step 4 for multiple rounds of CO_2 huff and puff.

3. Results

3.1. Effect of CO_2 in Degassed Crude Oil

Figure 4 shows the effect of CO_2 dissolved in degassed crude oil at various pressures. From Figure 4, the solubility of CO_2 in degassed crude oil shows a relatively clear positive linear correlation with pressure. As the saturation pressure increases, the solubility of CO_2 in degassed crude oil also increases. At a saturation pressure of 10.0 MPa, the solubility of CO_2 can reach 45.3 m^3/m^3, and the oil viscosity reduces to 894 mPa·s. This indicates that higher pressures can effectively enhance the dissolution effect of CO_2 in crude oil, which is beneficial for increasing oil expansion capacity and reducing viscosity.

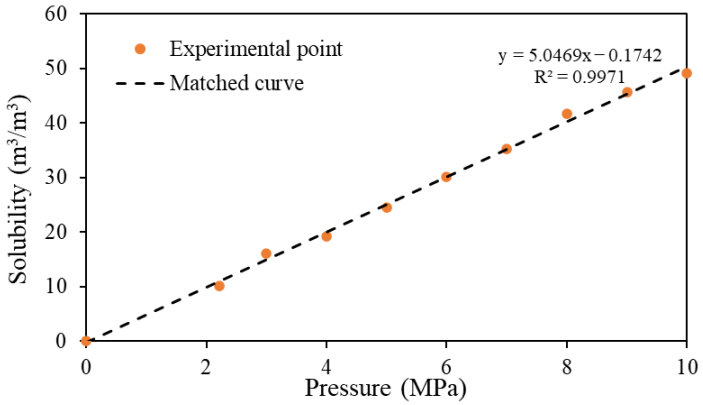


Figure 4. Effect of CO_2 dissolved in degassed crude oil at various pressures.

Figure 5 shows the effect of CO_2 viscosity reduction in degassed crude oil at varied solubilities. From Figure 5, the curve clearly reflects the exceptional performance of CO_2 dissolution in reducing the viscosity of heavy oil. When the solubility reaches 10.0 m^3/m^3, the oil viscosity is reduced by 20%. As the solubility increases to 49.0 m^3/m^3, the viscosity of the crude oil drops to 894 mPa·s. This significant enhancement in permeability aids

in reducing the extraction difficulties of medium and deep heavy oil, thus improving the effectiveness of development and increasing the crude oil recovery rate.

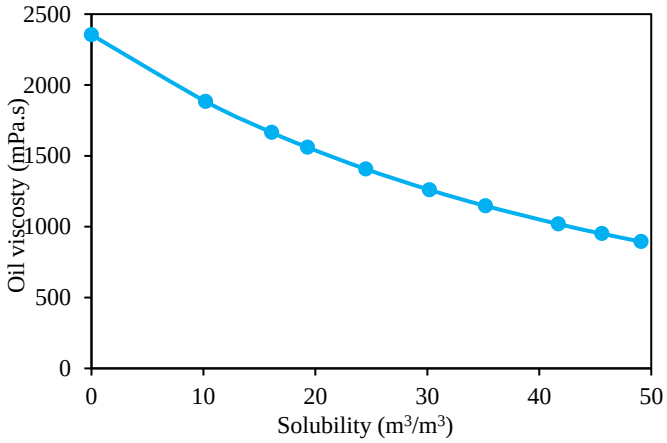


Figure 5. Effect of CO_2 viscosity reduction in degassed crude oil at various pressures.

3.2. Effect of CO_2 in Gas-Bearing Crude Oil

Figure 6 shows the original methane content for various saturation pressures. From Figure 6, the solubility of CH_4 in crude oil exhibits a positive linear correlation with saturation pressure. As the saturation pressure increases, the solubility of CH_4 in degassed crude oil also increases. At a saturation pressure of 10.0 MPa, the solubility of CH_4 in crude oil reaches 23.2 m^3/m^3. This indicates that the overall solubility of CH_4 in crude oil is weaker compared to CO_2.

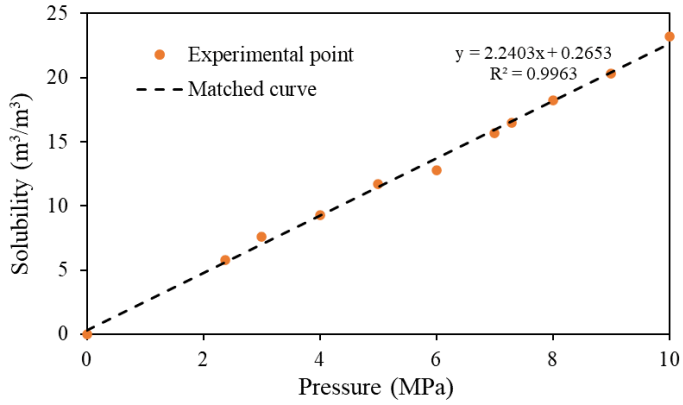


Figure 6. Original CH_4 content at various saturation pressures.

Figure 7 shows the effect of CO_2 dissolved in gas-bearing crude oil at various pressures. From Figure 7, crude oil saturated with CH_4 still has the capacity to further dissolve carbon dioxide CO_2. The increase in the solubility of CO_2 also shows a linear relationship with saturation pressure. When the saturation pressure reaches 10.0 MPa, the incremental solubility of CO_2 in the crude oil is 24.5 m^3/m^3, which even surpasses the original solubility of CH_4. This indicates that gases with higher solubility in crude oil exhibit a stronger competitive ability during co-solution.

Figure 8 shows the effect of CO_2 viscosity reduction in gas-bearing crude oil at various pressures. From Figure 8, the increased dissolution of CO_2 further reduces the viscosity of crude oil. When the additional solubility of CO_2 reaches 24.5 m^3/m^3 at 10 MPa, the viscosity of the crude oil decreases to 1161 mPa·s. This indicates that the hybrid viscosity-reducing effect of CO_2 in combination with CH_4 is more significant than that of a single gas.

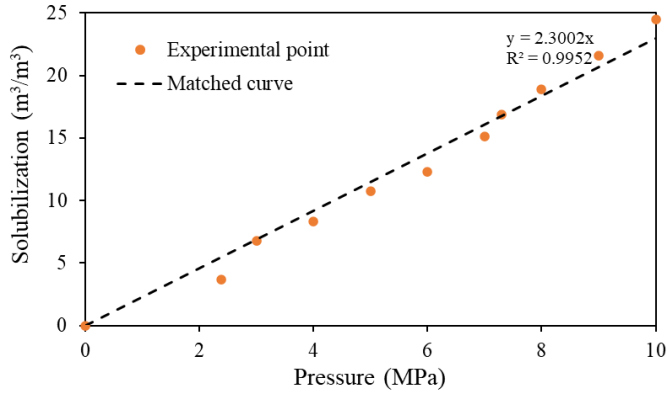


Figure 7. Effect of CO_2 dissolved in gas-bearing crude oil at various pressures.

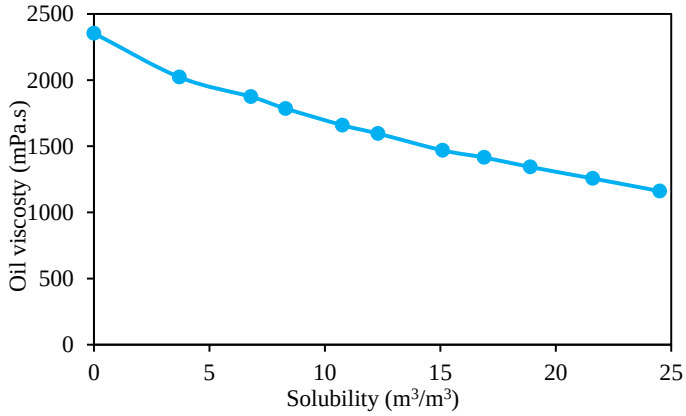
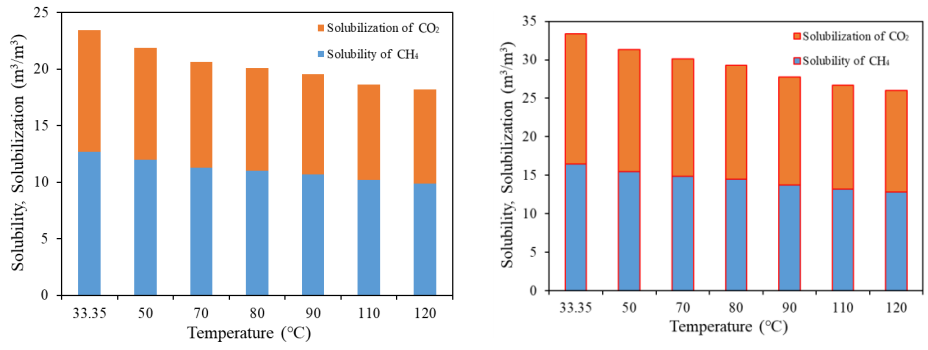


Figure 8. Effect of CO_2 viscosity reduction in gas-bearing crude oil at various pressures.

Figure 9 shows the effect of CO_2 dissolved in gas-bearing crude oil at various temperatures. From Figure 9, upon comparing the solubility of CH_4 and CO_2 in crude oil at different temperatures, it is evident that a higher temperature exerts a certain inhibitory effect on solubility. Bubbles are formed due to the increased molecular thermal motion at higher temperatures. At an experimental pressure of 5.0 MPa, when the temperature is raised from the reservoir temperature of 33.35 °C to 120 °C, the solubility of CH_4 and CO_2 in the crude oil decreases from 12.7 m^3/m^3 to 9.9 m^3/m^3 and from 10.8 m^3/m^3 to 8.3 m^3/m^3, respectively. At a reservoir pressure of 7.3 MPa, when the temperature increases from 33.35 °C to 120 °C, the solubility of CH_4 and CO_2 drops from 16.5 m^3/m^3 to 12.8 m^3/m^3 and from 16.9 m^3/m^3 to 13.2 m^3/m^3, respectively. This indicates that under high temperatures, CH_4 and CO_2 still retain a certain solubility, possibly due to the enhanced molecular diffusion capacity of gases in the oil phase at higher temperatures.



(**a**) Pressure = 5 MPa (**b**) Pressure = 7.3 MPa

Figure 9. Effect of CO_2 dissolved in gas-bearing crude oil at various temperatures.

3.3. Characterization of Dynamic Dissolution

Figure 10 shows the dissolution rate characteristic of CO_2 in gas-bearing crude oil. From Figure 10, initially, CO_2 exhibits a high dissolution rate of 0.009 $m^3/(m^3 \cdot min)$, and the gas-to-oil ratio increases rapidly. Subsequently, the dissolution rate of CO_2 drops sharply, eventually decreasing to 0.002 $m^3/(m^3 \cdot min)$. Due to the extended duration of the experiment, there were continuous environmental temperature changes. Therefore, gas exsolution phenomena were observed at some points, and the overall dissolution rate gradually decreased. Unlike the dissolution phenomena in degassed crude oil, the gas-to-oil ratio curve of the later stage was completely inconsistent with that of the earlier and middle stages, showing a notable decrease in dissolution capacity. This indicates that CO_2 can achieve efficient increased solubility effects within a relatively short period.

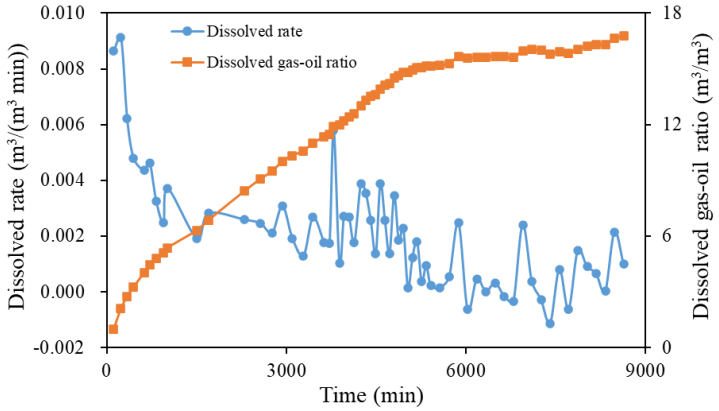


Figure 10. Dissolution rate characteristic of CO_2 in gas-bearing crude oil.

Figure 11 shows the pressure variation and diffusion characteristic of CO_2 in gas-bearing crude oil. From Figure 11, as the time goes on, the amount of dissolved gas gradually increases, and the system pressure decreases until it stabilizes. The equilibrium pressure stabilizes at approximately 13.0 MPa, with an overall pressure reduction of 2.01 MPa. Based on the matched curve from the semi-logarithmic linear graph of pressure drop versus time, the diffusion coefficient of CO_2 in gas-containing crude oil is calculated to be 8.62 $\times$ 10^{-7} m^2/s. This indicates that during the dynamic process, CO_2 still possesses a high molecular diffusion capability in gas-containing crude oil. CO_2 demonstrates good improvement in gas-bearing crude oil, and it is a favorable gas choice for enhancing oil recovery.

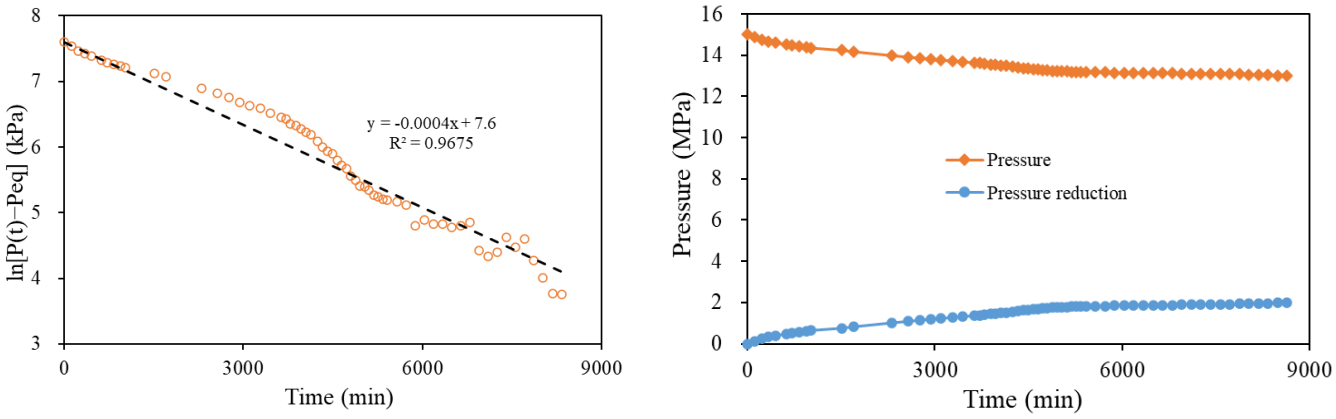


Figure 11. Pressure variation and diffusion characteristic of CO_2 in gas-bearing crude oil.

3.4. Effect on CO_2 Huff and Puff

The injection rate is a critical parameter affecting the efficiency of CO_2 huff and puff operations in medium and deep heavy oil reservoirs. It is generally believed that faster injection rates facilitate the formation of finger-like penetration, allowing CO_2 to reach deeper parts of the reservoir and dissolve more crude oil. However, the injection rate for each oil well should remain within the allowable injection pressure range of the reservoir. Figure 12 shows the comparison of CO_2 huff and puff effect of different injection rates. From Figure 12, initially, as the injection rate increases, both the oil production and the incremental oil production gradually increase. However, after reaching a certain value, the rate of increase in oil production begins to diminish. This indicates that there is an upper limit to the improvement of CO_2 huff and puff effectiveness due to the injection rate. Exceeding this limit may not result in proportionally greater increases in oil recovery.

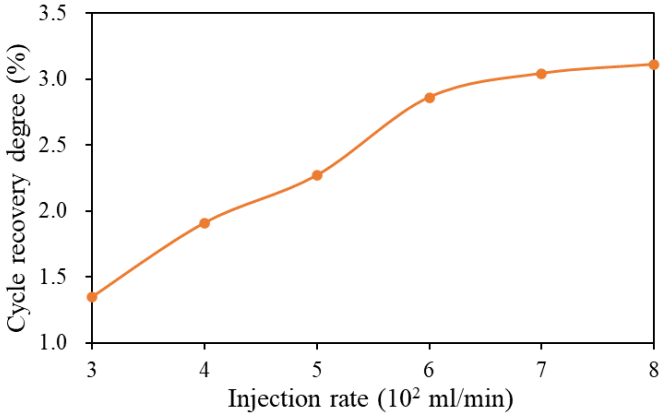


Figure 12. Comparison of CO_2 huff and puff effect of various injection rates.

A specified amount of CO_2 injected into medium and deep heavy oil reservoirs facilitates thorough contact with the crude oil, improving its properties and achieving the objective of enhanced production. Typically, the larger the periodic injection volume of CO_2, the greater the increase in oil production. However, the effectiveness of this production enhancement is not always directly proportional to the volume of CO_2 injected. Instead, there is an issue concerning the optimal injection volume, which needs to be identified to maximize recovery. Figure 13 shows the comparison of the CO_2 huff and puff effect of various injection volumes. From Figure 13, the more CO_2 injected cyclically into a reservoir, the greater the increase in oil production; however, the rate of increase diminishes over time. Beyond a certain injection volume, further increases in oil production tend to plateau. This plateau occurs because while increased injection volumes raise the formation pressure, thus enhancing oil expansion and viscosity reduction, there is a limit to these benefits. As the pressure reaches a certain threshold, the incremental increase in CO_2 solubility in the crude oil diminishes, thus inhibiting further improvement in CO_2 performance. This suggests an optimal balance in injection volumes that maximizes oil recovery while avoiding diminishing returns due to excessive pressure and limited solubility enhancements.

The soak time during CO_2 huff and puff operations significantly influences the dissolution and diffusion of CO_2, thereby affecting the overall development outcomes. Figure 14 shows the comparison of the CO_2 huff and puff effect at various soaking times. From Figure 14, when the soak time is relatively short, oil production increases with the extension of the soak time. However, after exceeding 90 min, the rate of increase gradually decreases, indicating that there is an optimal soak time for CO_2 huff and puff operations. This is because when the actual soak time is shorter than optimal, CO_2 does not have sufficient time to fully dissolve and diffuse, thus preventing its viscosity-reducing effects from being fully realized. When the soak time exceeds the optimal duration, extensive diffusion leads

to a significant drop in pressure, thus consuming the driving energy of the dissolved gas and reducing its effectiveness in mobilizing the crude oil.

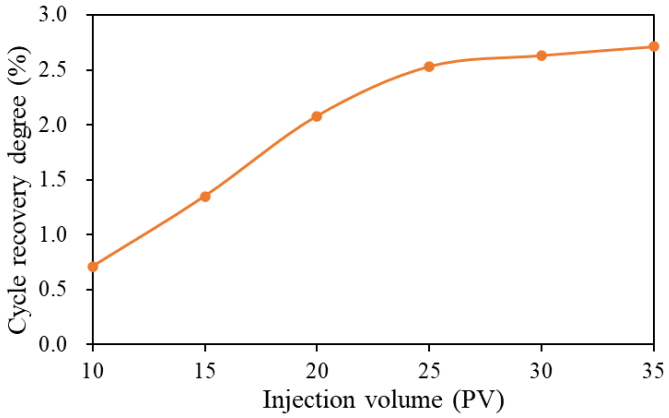


Figure 13. Comparison of CO_2 huff and puff effect of various injection volumes.

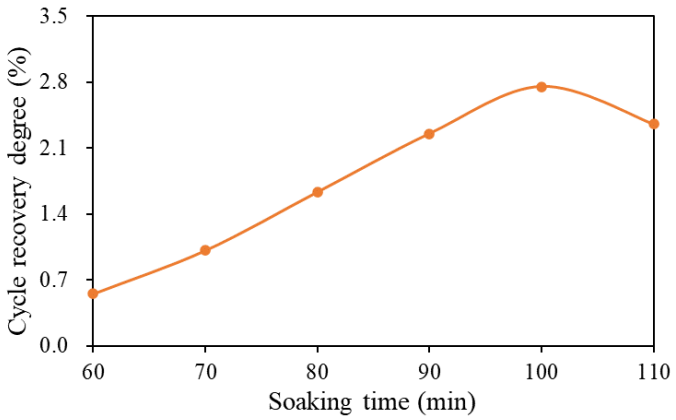


Figure 14. Comparison of CO_2 huff and puff effect at various soaking times.

The bottom hole pressure significantly impacts the solubility of CO_2 in crude oil. Figure 15 shows the comparison of the CO_2 huff and puff effect of various bottom hole pressures. From Figure 15, as the bottom hole pressure decreases, oil production initially increases. However, when the bottom hole pressure falls below 2.0 MPa, oil production begins to decline with further reductions in pressure. The analysis suggests that the bubble point pressure of the crude oil is about 2.0 MPa. When the bottom hole pressure is above this bubble point, a lower pressure enhances the production differential, thus improving the well drainage capacity. Additionally, the expansion of CO_2 dissolved in the crude oil at these pressures helps to reduce oil viscosity. However, once the bottom hole pressure drops below the bubble point pressure of crude oil, the CO_2 that was dissolved in the oil starts to escape, thus increasing the oil viscosity and the flow resistance, which in turn worsens production outcomes. Therefore, maintaining the bottom hole pressure slightly above the bubble point pressure of crude oil is considered optimal for enhancing oil recovery.

Figure 16 shows the comparison of the CO_2 huff and puff effect at various soaking times. From Figure 16, as the number of CO_2 huff and puff cycles increases, the content of saturated hydrocarbons in the crude oil rises, while the concentrations of aromatic hydrocarbons, resins, and asphaltenes decrease. This is because the injected CO_2 interacts with the crude oil, exhibiting a strong extraction capability for the lighter and medium components of the oil and less so for heavier components. Therefore, in CO_2 huff and puff operations, the output oil sees an increase in saturated hydrocarbons and a decrease in heavier components. As the number of cycles increases and the pressure further decreases, there is a significant loss of light components in the oil. Additionally, oil in regions far

from the well, constrained by its low flow properties, cannot flow back to the near-well areas. This results in progressively poorer huff and puff performance due to the inability to effectively mobilize and recover these distant oil resources.

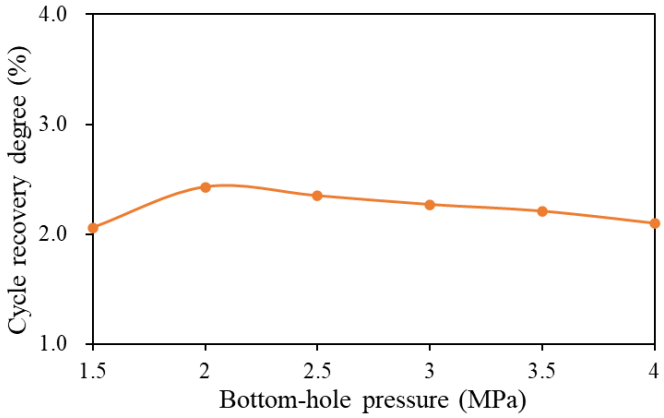


Figure 15. Comparison of CO_2 huff and puff effect of various bottom hole pressures.

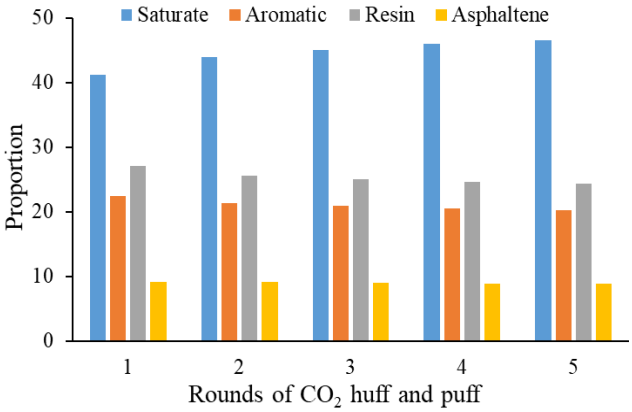


Figure 16. SARA fractions of heavy oil in various rounds of CO_2 huff and puff.

3.5. Economy of CO_2 Huff and Puff

Based on the detailed calculation, the cost of CO_2 huff and puff in field operation is USD 27–34/barrel oil. Variations in the injection rate, injection volume, soaking time, and bottom hole pressure will lead to different CO_2 performances, which will affect the cost of CO_2 huff and puff. In addition, the burial depth of the reservoir, the distance of the CO_2 carbon source, and other factors will also have a direct influence on the cost of oil production.

4. Conclusions

(1) The solubility of CO_2 in degassed crude oil is positively correlated with pressure. Higher pressures effectively enhance the solubility of CO_2, facilitating oil expansion and viscosity reduction. At a saturation pressure of 10.0 MPa, the solubility of CO_2 in crude oil can reach 49.1 m^3/m^3, and the oil's viscosity drops to 894 mPa·s.

(2) CO_2 with higher solubility in crude oil demonstrates stronger competitive abilities during co-solution. Crude oil saturated with CH_4 still retains the capacity to dissolve additional CO_2. At a saturation pressure of 10.0 MPa, the incremental solubility of CO_2 reaches 24.5 m^3/m^3. The hybrid effect of CO_2 and CH_4 allows for reducing the viscosity to 1161 mPa·s, which is slightly lower than the pure CO_2 dissolution case.

(3) Temperature exerts a restraining effect on solubility; as the temperature increases, molecular thermal motion intensifies, leading to gas exsolution. However, high tem-

peratures also enhance the molecular diffusion capabilities of gases in the oil phase, allowing CH_4 and CO_2 to maintain a certain level of solubility at elevated temperatures.

(4) CO_2 can achieve efficient incremental solubility effects within a short period. Initially, CO_2 has a high dissolution rate of 0.009 $m^3/(m^3 \cdot min)$, with a rapid increase in the gas-to-oil ratio. Subsequently, the dissolution rate of CO_2 sharply declines to 0.002 $m^3/(m^3 \cdot min)$, and its later dissolution capacity significantly decreases. During dynamic processes, CO_2 exhibits high molecular diffusion capabilities in gas-containing crude oil, with a diffusion coefficient of 8.62×10^{-7} m^2/s.

(5) For CO_2 huff and puff in medium to deep saturated heavy oil reservoirs, cyclic oil production is positively correlated with both the injection rate and the volume of CO_2, but the rate of increase gradually diminishes. Optimal injection rates and appropriate volumes should be determined in conjunction with the specific characteristics of the reservoir. Cyclic oil production initially increases with the extension of soaking time but eventually decreases, and there is an optimal soaking duration. The reduction of the bottom hole pressure can enhance the cyclic recovery rate, but it should remain above the bubble point pressure of the crude oil to prevent gas escape, resulting in the oil viscosity increasing and impairing the development effect. Moreover, due to the strong extraction capability of CO_2 for lighter components in crude oil, the content of saturates in the oil increases, while those of aromatics, resins, and asphaltenes decrease as the rounds of CO_2 huff and puff increase.

Author Contributions: X.S.: methodology, software, investigation, writing—original draft, writing—review and editing, visualization. Q.W.: resources, investigation, methodology. K.Z.: investigation, conceptualization, visualization. Y.W.: conceptualization, resources, funding. H.D.: conceptualization, supervision, project administration. J.Z.: conceptualization, supervision, resources. Y.Y.: investigation, project administration. All authors discussed the results and critically reviewed the manuscript. All authors have read and agreed to the published version of the manuscript.

Funding: The authors would like to acknowledge the financial support of Tianshan Talent Training Program and the Technology Project of CNPC (2023ZZ23-YJ06, 2023ZZ0405).

Data Availability Statement: Data presented in this study are available from the corresponding author upon reasonable request.

Conflicts of Interest: Authors Xiaorong Shi and Hong Dong were employed by Research Institute of Petroleum Exploration and Development, Xinjiang Oilfield Company, PetroChina. Authors Qian Wang and Yongbin Wu were employed by Research Institute of Petroleum Exploration and Development, PetroChina. Author Ke Zhao was employed by Heavy Oil Recovery Branch of Xinjiang Oilfield Company, PetroChina. The remaining authors declare that the research was conducted in the absence of any commercial or financial relationships that could be construed as a potential conflict of interest.

References

1. Lu, C.; Liu, H.; Zhao, W.; Lu, K.; Liu, Y.; Tian, J.; Tan, X. Experimental investigation of in-situ emulsion formation to improve viscous-oil recovery in steam-injection process assisted by viscosity reducer. *SPE J.* **2016**, *22*, 130–137. [CrossRef]
2. Zhao, D.; Wang, J.; Gates, I. Optimized solvent-aided steam-flooding strategy for recovery of thin heavy oil reservoirs. *Fuel* **2013**, *112*, 50–59. [CrossRef]
3. Yuan, S.Y.; Wang, Q. New progress and prospect of oilfields development technologies in China. *Pet. Explor. Dev.* **2018**, *45*, 698–711. [CrossRef]
4. Fang, J.C.; Li, X.Q.; Ji, B.Y.; Wang, H.B.; Lu, X. Prospect of replacement technology for enhanced oil recovery after cyclic steam stimulation of heavy oil in China. *Fault-Block Oil Gas Field* **2022**, *29*, 378–382.
5. Liu, W.Z. *Development Model of Thermal Recovery Heavy Oil Reservoir*; Petroleum Industry Press: Beijing, China, 1998.
6. Zhang, F.L.; Zhao, H.Y. *Development Technology of Heavy Oil Steam Injection in Liaohe Oilfield*; Petroleum Industry Press: Beijing, China, 2007.
7. Wang, L.J.; Liu, X.Y.; Chen, W.Q.; Lv, Y.Q. Research and application of steam enhancer in super heavy oil reservoir of Dan 56 oilfield. *J. Oil Gas Technol.* **2009**, *31*, 357–367.
8. Cao, Y.B.; Liu, D.Q.; Wang, S.T.; Yu, T.T.; Zhang, Z.P. Three-dimensional physical simulation and application of chemical-assisted steam flooding in medium and deep heavy oil reservoirs. *Acta Pet. Sin.* **2014**, *35*, 739–744.

9. Cao, Y.B.; Liu, D.Q.; Zhang, Z.P.; Wang, S.T.; Wang, Q.; Xia, D.H. Steam channeling control technology of super heavy oil steam flooding in Shengli Oilfield. *Pet. Explor. Dev.* **2012**, *39*, 785–790. [CrossRef]
10. Yang, Z.C.; Lu, Y.B.; Yang, G.; Huang, C.; Ge, D.L.; Jia, S.; Wu, Y.B.; Wang, G.Q. Pre-CO_2 energy storage fracturing technology in horizontal wells for medium-to-deep heavy oil. *Lithol. Reserv.* **2024**, *36*, 178–184.
11. Lotfollahi, M.; Farajzadeh, R.; Delshad, M.; Al-Abri, A.-K.; Wassing, B.M.; Al-Mjeni, R.; Awan, K.; Bedrikovetsky, P. Mechanistic Simulation of Polymer Injectivity in Field Tests. *SPE J.* **2016**, *21*, 1178–1191. [CrossRef]
12. Sohrabi, M.; Jamiolahmady, M.; Al-Quraini, A. Heavy oil recovery by liquid CO_2/water injection. In Proceedings of the EUROPEC/EAGE Conference and Exhibition, London, UK, 11–14 June 2007.
13. Wang, C. Research on Percolation Mechanism in Superdeep Heavy Oil Reservoir with Fractured Well by CO_2 Huff and Puff. Master's Thesis, Southwest Petroleum University, Chengdu, China, 2017.
14. Zhang, J.; Zhou, L.F.; Zhang, X.H.; Zhang, M.L.; Fan, J.; Du, H.B. Effects of CO_2 huff and puff in horizontal wells in shallow-burial thin heavy oil reservoirs. *Xinjiang Pet. Geol.* **2018**, *39*, 485–491.
15. Haskin, H.K.; Alston, R.B. An evaluation of CO huff-n-puff tests in Texas. *J. Pet. Technol.* **1989**, *41*, 177–184. [CrossRef]
16. Monger, T.G.; Comaj, M.A. Laboratory and field evaluation of the CO_2 huff-n-puff process for light-oil recovery. *SPE Reserv. Eng.* **1988**, *3*, 1168–1176. [CrossRef]
17. Schenewerk, P.A.; Thomas, J.; Bassiouni, Z.A.; Wolcott, J. Evaluation of a south Louisiana CO_2 huff-n-puff field test. In Proceedings of the SPE/DOE Enhanced Oil Recovery Symposium, Tulsa, OK, USA, 22–24 April 1992; pp. 417–421.
18. Wehner, S.C. CO_2 huff-n-puff: Initial results from a waterflood SSC reservoir. In Proceedings of the Permian Basin Oil and Gas Recovery Conference, Midland, TX, USA, 27–29 March 1996; pp. 613–622.
19. Wang, S.L.; Sun, B.C.; Wang, L.; Li, Z.R.; Yang, J. Study and application of the stimulation mechanism of CO_2 huff and puff. *Drill. Prod. Technol.* **2004**, *27*, 98–101.
20. Luo, C. Research and application of quasi-dry CO_2 fracturing technology. *Chem. Eng. Oil Gas* **2021**, *50*, 83–87.
21. Ding, Y.; Ma, X.X.; Ye, L.; Xiao, Y.L.; Zhang, Y.M.; Gu, Y.H.; Ma, C.X. Rock breaking mechanism of CO_2 and fracturing technology. *Lithol. Reserv.* **2018**, *30*, 151–159.

Disclaimer/Publisher's Note: The statements, opinions and data contained in all publications are solely those of the individual author(s) and contributor(s) and not of MDPI and/or the editor(s). MDPI and/or the editor(s) disclaim responsibility for any injury to people or property resulting from any ideas, methods, instructions or products referred to in the content.